TU/e EINDHOVEN UNIVERSITY OF TECHNOLOGY

The effect of electrolytic gas evolution on mass transfer at electrodes

Citation for published version (APA):
Janssen, L. J. J., & Barendrecht, E. (1979). The effect of electrolytic gas evolution on mass transfer at electrodes. *Electrochimica Acta*, *24*(6), 693-699. https://doi.org/10.1016/0013-4686(79)87053-X

DOI:
10.1016/0013-4686(79)87053-X

Document status and date:
Published: 01/01/1979

Document Version:
Publisher's PDF, also known as Version of Record (includes final page, issue and volume numbers)

Please check the document version of this publication:

• A submitted manuscript is the version of the article upon submission and before peer-review. There can be important differences between the submitted version and the official published version of record. People interested in the research are advised to contact the author for the final version of the publication, or visit the DOI to the publisher's website.
• The final author version and the galley proof are versions of the publication after peer review.
• The final published version features the final layout of the paper including the volume, issue and page numbers.

Link to publication

General rights
Copyright and moral rights for the publications made accessible in the public portal are retained by the authors and/or other copyright owners and it is a condition of accessing publications that users recognise and abide by the legal requirements associated with these rights.

• Users may download and print one copy of any publication from the public portal for the purpose of private study or research.
• You may not further distribute the material or use it for any profit-making activity or commercial gain
• You may freely distribute the URL identifying the publication in the public portal.

If the publication is distributed under the terms of Article 25fa of the Dutch Copyright Act, indicated by the "Taverne" license above, please follow below link for the End User Agreement:

www.tue.nl/taverne

Take down policy
If you believe that this document breaches copyright please contact us at:

openaccess@tue.nl

providing details and we will investigate your claim.

Download date: 07. Jul. 2024

Electrochimica Acta, Vol. 24, pp. 693–699.
© Pergamon Press Ltd. 1979. Printed in Great Britain.
0019–4686/79/0601–0693 $02.00/0

THE EFFECT OF ELECTROLYTIC GAS EVOLUTION ON MASS TRANSFER AT ELECTRODES

L. J. J. JANSSEN and E. BARENDRECHT
Department of Electrochemistry, Eindhoven University of Technology, Postbus 513, Eindhoven, The Netherlands

(*Received* 31 *March* 1978; *in revised form* 21 *December* 1978)

Abstract – A theoretical description of a hydrodynamic model for mass transfer at gas evolving electrodes where no coalescence of gas bubbles occurs is given. To elucidate the mechanism of mass transfer, the thickness of the Nernst diffusion layer, δ, has been determined as a function of the volumetric rate of the gas evolution, v, for both a gas evolving disc electrode and non-gas evolving ring electrodes placed concentrically around the gas evolving disc electrode. These experiments are performed for both hydrogen and oxygen evolution in alkaline solution.

It is found that for the hydrogen evolving electrode, where no coalescence occurs, the slope of the $\log \delta/\log v$ curve agrees with the theoretical slope. For the oxygen evolving electrode, where coalescence occurs frequently, the experimental and the theoretical slope differ markedly.

NOMENCLATURE

- c concentration of the indicator ion in the bulk of the electrolyte (mol cm^{-3})
- C_m constant factor
- d diameter of a bubble (cm)
- d_b diameter of a bubble departing from a horizontal gas evolving electrode, *ie* break-off diameter of a bubble (cm)
- D diffusion coefficient of an indicator ion (cm^2 s^{-1})
- f frequency of bubble emission from an active site on the electrode surface (s^{-1})
- F Faraday constant (C mol^{-1})
- g acceleration due to gravity (cm s^{-2})
- Gr Grashof number ($Gr = gx^3(\rho_0 - \rho_i)\nu^{-2}\rho_i^{-1}$)
- i current density (mA cm^{-2})
- i_p current density of the reduction or oxidation of an indicator ion p (mA cm^{-2})
- k mass transfer coefficient (cm s^{-1})
- l length of the electrode in the direction of the flow
- n number of active sites per unit surface (cm^{-2})
- Nu Nusselt number ($Nu = k \times D^{-1}$)
- Sc Schmidt number ($Sc = \nu D^{-1}$)
- T absolute temperature (K)
- x characteristic dimension (cm)
- U velocity of the solution (cm s^{-1})
- v volumetric rate of the gas phase per unit surface, *ie* superficial velocity of the gas (cm s^{-1})
- v_t terminal velocity of bubble rise (cm s^{-1})
- z drag coefficient, *ie* the ratio between the volume of the liquid transported upwards by rising bubbles and the volume of the rising bubbles
- δ thickness of the Nernst diffusion layer (cm)
- ρ mass density (g cm^{-3})
- ε volumetric gas fraction in the bubble street of the gas evolving horizontal electrode
- η dynamic viscosity of the liquid (g cm^{-1} s^{-1})
- ν kinematic viscosity of the liquid (cm^2 s^{-1})

Subscripts

- g gas
- l liquid
- 0 bulk of the solution
- i electrode/solution interface.

1. INTRODUCTION

The study of mass transfer at gas evolving electrodes is of great interest, especially for the electrochemical industry and the subject has been investigated intensively during the last 15 years.

In a recent thesis of Vogt[1] a comprehensive survey of experimental and theoretical results is given. Vogt has deduced a theoretical equation in dimensionless numbers for mass transfer at gas evolving electrodes similar to the dimensional form of those of Ibl and Venczel[4–7].

In a recent paper Janssen[2] has concluded that the mass transfer can be explained on the basis of the hydrodynamic model, first proposed in 1973[3], when no coalescence of gas bubbles occurs. According to Janssen[2] the penetration model of Ibl and Venczel[4–7] may be useful when coalescence of gas bubbles occurs frequently.

In this article, the hydrodynamic model is described quantitatively. The theoretical relation between δ and the volumetric rate of gas evolution for a gas evolving electrode is compared with the experimental one for both the hydrogen and the oxygen evolving electrode in alkaline solution.

To check the conclusions about the mechanism of mass transfer at gas evolving electrodes, δ is determined at ring electrodes placed concentrically to a gas evolving disc. The solution flow induced by ascending gas bubbles determines δ at the ring electrodes. Moreover, the relation between δ at the ring electrode and δ at the gas evolving electrode is determined.

2. EXPERIMENTAL

2.1 *Electrolytic cell*

A normal H-type electrolytic cell divided into two compartments separated by an ion-exchange membrane (Nafion 425) was used. A diagram of this cell

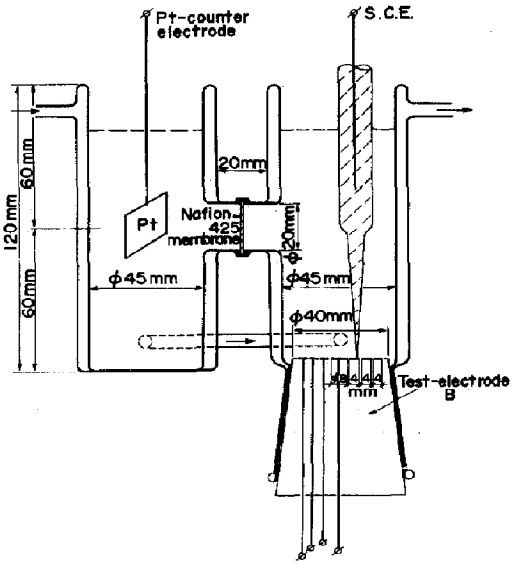

Fig. 1. Schematic diagram of the experimental cell.

with pertinent dimensions is given in Fig. 1. The horizontal test-electrode (dia 4.0 cm) served as a part of the bottom of the test-compartment. The electrolytic cell was thermostatted; the temperature of the electrolyte was usually 25°C.

2.2 *Electrodes*

Two different types of electrode, A and B, were used. Both types of electrode consisted of a nickel disc of about 0.8 cm dia surrounded concentrically by nickel rings of different surface area. The disc and the rings were separated from one another by an insulating material of a thickness of about 0.006 cm (Fig. 1).

For electrode A the surface area of the disc was 0.51 cm^2, that of the inner ring 0.35 cm^2 and that of the outer ring 4.07 cm^2. The width of the inner ring was 0.115 cm and that of the outer ring 0.72 cm. For electrode B the surface area of the disc was 0.55 cm^2, that of the inner ring 1.79 cm^2, that of the middle ring 2.98 cm^2 and that of the outer ring 4.36 cm^2. The width of all of these three rings was about 0.4 cm. A diagram of electrode B is shown in Fig. 1.

2.3 *Electrolyte and analysis*

A 1 M KOH solution was used as supporting electrolyte, unless otherwise mentioned. For the experiments with the hydrogen evolving electrode the solution was made 0.03 M in $K_3Fe(CN)_6$. For the experiments with the oxygen evolving electrodes the 1 M KOH solution contained 0.03 M $K_4Fe(CN)_6$.

When, however, the thickness of the diffusion layer at the non-gas evolving electrodes had to be determined, the alkaline solution was made 0.03 M in $K_3Fe(CN)_6$. The use of these different indicator ions was preferred because of the small difference between the normal potential of the $Fe(CN)_6^{4-}/Fe(CN)_6^{3-}$ redox couple and that of the O_2/OH^- redox couple in 1 M KOH. The quantity of $Fe(CN)_6^{3-}$ formed during the oxygen evolution was determined by titration with Ce^{4+} [8].

2.4 *Procedure*

Usually, the following procedure was applied in determining the thickness of the Nernst diffusion layer at a gas evolving electrode.

Before each experiment in a series, the test electrode was polarized in the supporting electrolyte for 15 min at a current density equal to that of the experiment. After the 15 min pre-polarization a calculated quantity of the indicator ion was added.

Usually 10 ml 0.63 M $K_3Fe(CN)_6$ or $K_4Fe(CN)_6$ was added to 175 ml supporting electrolyte.

The determination started without interrupting the current at the addition of the indicator ion.

During a series of experiments the determinations were performed in a sequence of decreasing current density. The decrease in the concentration of the indicator ion was about 2%.

In a number of experiments, however, the current was just switched on at the moment of addition of the indicator ion.

The thickness of the diffusion layer at the non-gas evolving ring electrodes was obtained by measuring the current used for the reduction of $Fe(CN)_6^{4-}$ for all experiments.

For the experiments with the hydrogen and the oxygen evolving electrodes, the potential of one or all the non-gas evolving ring electrodes was maintained potentiostatically at -500 mV and -300 mV *vs sce*, respectively. At these potentials the oxidation of hydrogen was negligible and the limiting diffusion current for the reduction of $Fe(CN)_6^{3-}$ was attained. The current at the gas evolving electrode, however, was adjusted galvanostatically. For 3 min this electrode was polarized with a constant current density. During this period the current at the non-gas evolving electrode was recorded. The average current for the last minute of this period was determined.

Usually a series of experiments started with the highest current density; the current at the disc was decreased in steps. After measurements with decreasing current density, measurements with increasing current density were carried out in a limited number of experiments. The results were practically the same.

3. RESULTS

3.1 *Introduction*

The thickness δ of the Nernst diffusion layer is calculated from the well-known equation:

$$\delta = \frac{FDc}{i_p}.$$

For the calculation of δ the diffusion coefficient of $Fe(CN)_6^{4-}$ *vz* 7.0×10^{-6} cm^2/s at 25°C and that of $Fe(CN)_6^{3-}$ 7.9×10^{-6} cm^2/s at 25°C were used[3]. Taking into account the activation energy of the diffusion coefficient of the indicator ion in 1 M KOH[9] and the viscosity of KOH solutions[10] the diffusion coefficients of the indicator ions at different temperatures and solutions with different KOH-concentrations were calculated. The thickness of the diffusion layer at both the gas evolving electrode and the non-gas evolving electrodes was usually deter-

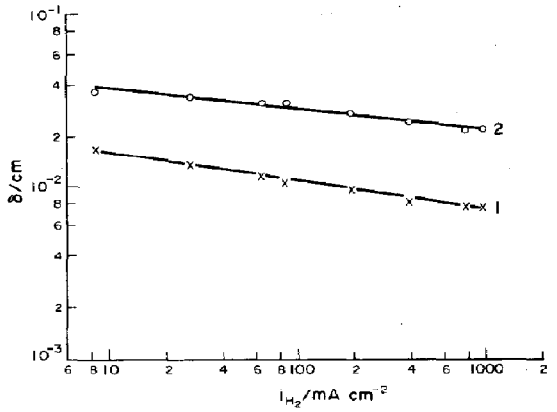

Fig. 2. Plot of log δ at the inner (1) and the outer (2) ring *vs* log i_{H_2} at the disc of electrode A. The rings were polarized separately.

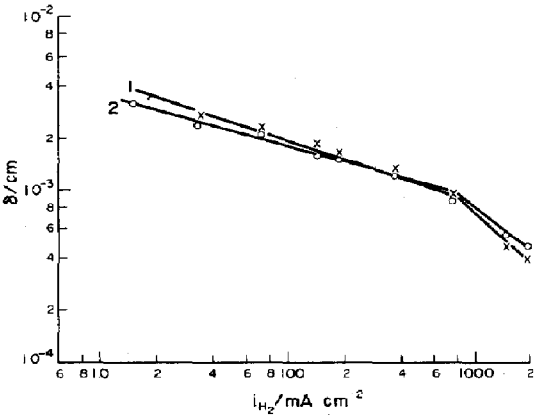

Fig. 4. Plot of log δ *vs* log i_{H_2} at the disc electrode A with prepolarization for 15 min (curve 1) and without prepolarization (curve 2).

mined as a function of the current density used for the gas evolution. In the next section relations between δ and i_{O_2} or i_{H_2} are given.

3.2 *Hydrogen evolution*

The bubbles ascending from the disc electrode induce an electrolyte flow in the cell. This flow also passes the ring electrodes mounted concentrically around the gas evolving disc electrode.

In the following the influence of the rate of the hydrogen evolution upon the limiting rate of mass transfer at the non-gas evolving electrodes is shown.

In Fig. 2, log δ at both rings of electrode A is plotted *vs* log i_{H_2} at the disc, when the rings are polarized separately at -500 mV. The current density $i_{H_2} = i - i_{Fe(CN)_6^{3-}}$. For the experiments where both rings of electrode A where polarized simultaneously, it was found that the slopes of the log δ/log i_{H_2} curves were equal to those of Fig. 2, δ for the outer ring was equal to that of Fig. 2 and δ for the inner ring was a factor 1.8 greater than that of Fig. 2.

The results for electrode B at separate polarization of the ring electrodes are represented in Fig. 3. This figure shows that δ increases with increasing distance between the ring and the gas evolving disc electrode. From experiments with separate and with simultaneous polarization, it was found that for simultaneous polarization, δ at the inner and the middle ring reaches a higher value and δ at the outer ring equals the value obtained at separate polarization. This result can be explained by the decrease of the $Fe(CN)_6^{3-}$ concentration in the electrolyte flowing past the outer ring. It was also determined for the inner ring of electrode A when the hydrogen evolution occurred with the same current density at both the outer ring and the disc.

Additional hydrogen evolution at the outer ring had a small influence upon δ at the inner ring, *viz* at $i_{H_2} = 100$ mA/cm^2, δ decreased about 15% and the slope of the log δ/log i_{H_2} curve increased about 50%.

The influence of temperature upon δ at the inner ring of electrode A, at a constant volumetric rate of hydrogen and water vapour formation on the disc electrode, was determined. It appeared that in the investigated temperature range from 25 to 70°C (and at a volumetric rate of hydrogen and water vapour

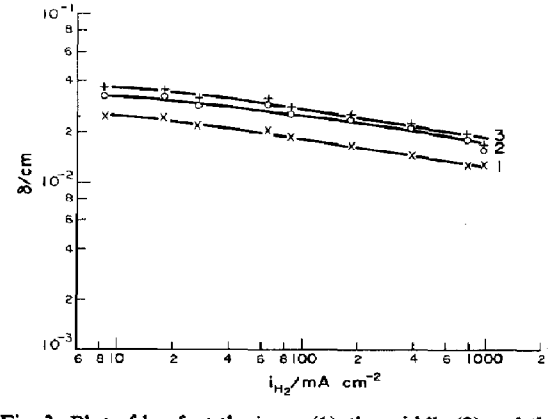

Fig. 3. Plot of log δ at the inner (1), the middle (2) and the outer (3) ring *vs* log i_{H_2} at the disc of electrode B. The rings were polarized separately.

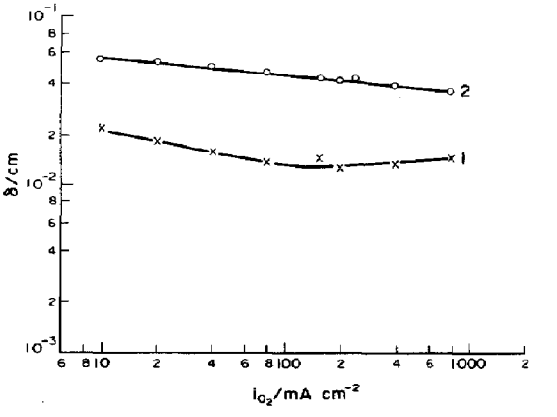

Fig. 5. Plot of log δ at the inner (1) and the outer (2) ring *vs* log i_{O_2} at the disc of electrode A. The rings were polarized separately.

formation of 0.77 ml/min cm^2, corresponding with a hydrogen evolution of 200 mA/cm^2 at 25°C), the temperature has practically no influence upon δ. The effect of the KOH-concentration upon δ was also investigated at the inner ring of electrode A at 25°C and at a hydrogen evolution of 40 mA/cm^2 on the disc. Solutions of 1, 2, 3 and 4 M KOH containing 0.03 M $K_4Fe(CN)_6$ were used.

It appeared that δ increased slightly with increasing KOH-concentration; δ at 4 M KOH is about 20% larger than δ at 1 M KOH.

For the hydrogen evolving disc electrode $\log \delta/\log i_{H_2}$ curves are plotted in Fig. 4. This figure shows also the influence of the 15 min pre-polarization of the disc electrode. The experiments were started at the highest current density. In both experiments at $i_{H_2} > 1.5$ A/cm^2 coalescence of hydrogen bubbles occurred very frequently.

3.3 *Oxygen evolution*

During oxygen evolution at the disc electrode, the reduction current of $Fe(CN)_6^{3-}$ at the ring electrode fluctuated little at current densities for the disc electrode, $i_{O_2} < 80$ mA/cm^2, but intensively at higher current densities, $i_{O_2} > 80$ mA/cm^2.

The change occurred rather abruptly and was not observed with hydrogen evolution. This abrupt change may be caused by the sudden occurrence of frequent coalescence of oxygen bubbles at $i_{O_2} = 80$ mA/cm^2.

In the following the influence of the rate of oxygen evolution upon δ of the ring electrodes is shown. In Fig. 5, $\log \delta$ at the two rings of electrode A is plotted *vs* $\log i_{O_2}$ at the disc for separate polarization of both rings at -300 mV. The results for electrode B are given in Fig. 6, which shows that δ also increases with increasing distance between ring and gas evolving disc for separate polarization of the ring electrodes.

The effect of the simultaneous polarization of the ring electrodes upon δ was the same as with the hydrogen evolving electrodes.

δ was also determined at the inner ring of electrode A for simultaneous oxygen evolution at both the disc and the outer ring with the same current density. The additional oxygen evolution at the outer ring decreased δ at the inner ring with about 30%.

For the investigated current density range from 10 to 400 mA/cm^2 the slope of the relation between $\log \delta$ at the inner ring and $\log i_{O_2}$ at the disc and at the outer ring is equal to that at $i_{O_2} < 80$ mA/cm^2, Fig. 5.

The relation between $\log \delta$ and $\log i_{O_2}$ for the gas evolving disc electrode A is represented in Fig. 7. In this case, $Fe(CN)_6^{4-}$ was used as indicator ion and was oxidized at the limiting current density.

For the oxygen evolving electrode $i_{O_2} = i - i_{Fe(CN)_6^{4-}}$. The $\log \delta/\log i_{O_2}$ curve of Fig. 7 has an intersection point at about 20 mA/cm^2. At high current densities, *viz* $i_{O_2} > 20$ mA/cm^2, the slope is much steeper than those of the curves of Figs 5 and 6.

4. THEORY

A gas bubble is initiated on an active site of the electrode, and grows by absorption of gas from the surrounding supersaturated solution. Upon detachment each ascending gas bubble transports upwards a quantity of solution.

At steady state the volume of the liquid transported upwards is equal to the volume of the liquid which flows downwards. The velocity distribution of the latter flow depends on many factors, such as the dimensions of the electrolytic cell and of the gas evolving electrode, the position of the gas evolving electrode, the volumetric rate of the gas evolution, the size of the ascending bubbles and the viscosity of the liquid. The electrolyte flow induced by ascending bubbles strongly affect each other, and the trajectory of the ascending bubble.

The hydrodynamic model introduced by Janssen and Hoogland[3] is based on the liquid flow induced by ascending gas bubbles. This flow can be compared with the free-convection flow induced by differences in density of the electrolyte.

For both turbulent and laminar free-convection flow, experimental as well as theoretical relations have been found for mass transfer at both vertical and horizontal electrodes[11–14]. However, an exact or even approximate theoretical treatment of the hydrodynamic model of Janssen and Hoogland for the mass transfer is not available. Only some experimental relations for related systems have been obtained.

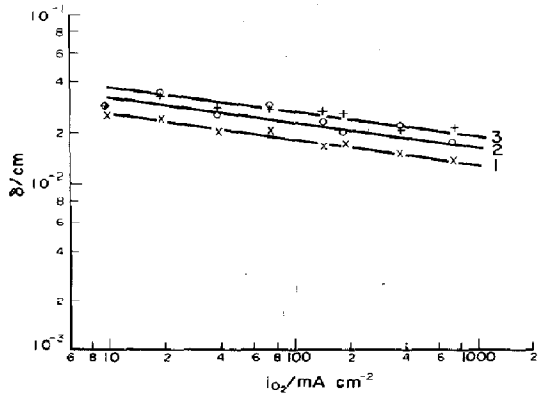

Fig. 6. Plot of $\log \delta$ at the inner (1), the middle (2) and the outer (3) ring *vs* $\log i_{O_2}$ at the disc of electrode B. The rings were polarized separately.

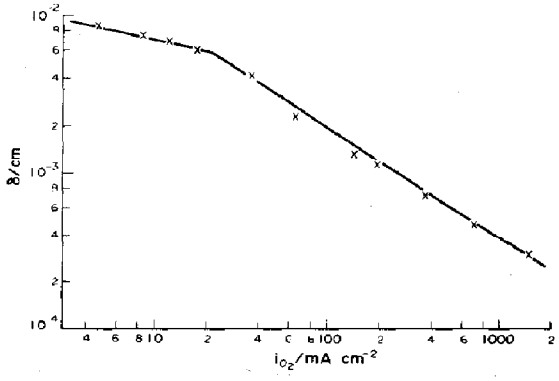

Fig. 7. Plot of $\log \delta$ *vs* $\log i_{O_2}$ at the disc of electrode A.

Ibl *et al*[15, 16] have investigated mass transfer at vertical electrodes when gas bubbles were sparged by porous frittes at the bottom of the electrolytic cell into the electrolyte. A great part of these gas bubbles ascend in the vicinity of the vertical electrode. Weder[17] studied mass transfer at a horizontal electrode where gas was bubbled through a hole in the centre of the electrode.

Free-convection flow due to differences in density of the liquid is turbulent for disc electrodes with diameters greater than about 1–2 cm[11]. For this turbulent flow the mass transfer rate at the electrode is given by[11],

$$Nu = 0.15(Gr \,.\, Sc)^{1/3}. \tag{1}$$

Substitution of k/D by δ, the thickness of the Nernst diffusion layer, gives

$$\delta = 6.7\left(\frac{\rho_l \nu D}{(\rho_0 - \rho_l)g}\right)^{1/3}. \tag{2}$$

For free-convection flow, resulting from differences in density of the liquid, the buoyancy force per unit mass is

$$\frac{(\rho_0 - \rho_l)g}{\rho_l}.$$

For reasons of analogy we considered a horizontal gas evolving disc electrode. In this case the convection flow is only caused by the lift effect of ascending gas bubbles.

Assuming that both the volumetric gas fraction, ε, in the bubble street and the drag coefficient, z, are independent of the height above the electrode surface, the buoyancy factor per unit mass i:

$$(z\varepsilon\rho_1 g)/[(1-\varepsilon)\rho_1 + \varepsilon\rho_g].$$

This factor is similar to the buoyancy factor resulting from differences in density of the solution.

Consequently, the factor $(\rho_0 - \rho_l)/\rho_l$ in (2) is replaced by

$$z\varepsilon\rho_1/[(1-\varepsilon)\rho_1 + \varepsilon\rho_g].$$

This gives the following expression for δ

$$\delta = C_1\left(\frac{\nu D[(1-\varepsilon)\rho_1 + \varepsilon\rho_g]}{z\varepsilon\rho_1 g}\right)^{1/3}. \tag{3}$$

The detached bubbles rise in a swarm and induce a liquid flow. This flow affects both the trajectory and the velocity of each bubble. Assuming an equal size of all the bubbles the relation between the superficial velocity of the gas – the volumetric rate, v, of the gas phase per unit of surface area – and the volumetric gas fraction, ε, is given[18] by

$$v = v_t\left(\frac{\varepsilon}{1-\varepsilon}\right). \tag{4}$$

In this equation v_t is the terminal velocity of a single bubble in an infinite medium and is equal to

$$v_t = \frac{1}{12} g d^2 \frac{(\rho_1 - \rho_g)}{\eta_1}. \tag{5}$$

Rietema *et al*[18] studied a system similar to a gas evolving horizontal electrode.

Relation (4) is also found for a "turbulent" regime of ascending bubbles[19]. This regime is characterized by large liquid convection induced by ascending bubbles. The "turbulent" regime, mentioned in the literature, is associated with bubble coalescence. However, we consider now a regime where no coalescence of bubbles occurs. This should be well compared with a "laminar" regime as defined by Zuber[19]. In contrast to our bubble system, however, in the system with "laminar" flow the liquid ahead of and behind rising bubbles is at rest; no gross liquid circulation exists[19]. For the "laminar" regime Zuber gives

$$v = v_t\varepsilon(1-\varepsilon). \tag{6}$$

At low volumetric gas fractions v is practically equal to $v_t\varepsilon$ for both regimes of the bubble system.

Owing to the influence of liquid flow upon the behaviour of bubbles, (4) for the relation between v and v_t is preferable.

Taking into account $\rho_g \ll \rho_1$ substitution of (4) into (3) gives

$$\delta = C_1\left(\frac{\nu D v_t}{zgv}\right)^{1/3}. \tag{7}$$

Assuming the drag coefficient z does not depend on v, from (7) it can be deduced that the log δ/log v curve is straight with a slope of -0.33.

For a population density, n, of active sites on the electrode, a frequency, f, of bubble emission at an active site and a break-off diameter, d_b, the volumetric rate of gas evolution per unit of surface area is

$$v = \frac{1}{6}\pi d_b^3 nf. \tag{8}$$

From (6) and (7) it follows after substitution of $(\rho_1 - \rho_g)/\eta \approx \rho_1/\eta = \nu$ that

$$\delta = C_2\left(\frac{D}{zd_b nf}\right)^{1/3}. \tag{9}$$

If the uniform bubble diameter d_b depends on v, it is likely also that the parameters z, n and f depend on v. The relation between δ and v is then complex.

Zuber[19] has deduced a relation for heat transfer at a horizontal surface at which nuclear boiling occurs. Owing to the analogy between heat and mass transfer the relation of Zuber can be transformed into a relation for mass transfer. In this case only the effect of bubbles is taken into account. After substitution of various parameters by the analogues for mass transfer we obtain (and assuming $\rho_g \ll \rho_1$)

$$\frac{kd}{D} = C_3\left(\frac{gd^3\varepsilon}{\nu D}\right)^{1/3}. \tag{10}$$

Substitution of k by D/δ and rearrangement of (10) gives

$$d = C_4\left(\frac{\nu D}{g\varepsilon}\right)^{1/3}. \tag{11}$$

As mentioned earlier, $\varepsilon = v/v_t$ at low gas fractions. From this relation and (11) it follows that

$$\delta = C_4\left(\frac{\nu D v_t}{gv}\right)^{1/3}. \tag{12}$$

Comparison of this equation for δ with (7) shows that both equations for δ are equal if $C_4 = C_2 z^{-1/3}$.

5. DISCUSSION

During both the hydrogen and the oxygen evolution at the disc electrode a circulation flow of the solution occurs in the electrolytic cell. The rate of this flow increases with increasing rate of gas evolution. Due to this increasing flow rate δ decreases at the ring electrodes, placed concentrically around the gas evolving disc electrode.

Assuming that the effect of the edges can be neglected, the thickness δ of the Nernst diffusion layer according to Levich for a plate electrode in laminar flow is[20]

$$\delta = 1.47 D^{1/3} l^{1/2} \nu^{1/6} U^{-1/2}. \qquad (13)$$

The solution flow velocity U at the inner ring of electrode A is calculated for hydrogen evolution of 1 A/cm^2 at the disc of electrode A at 25°C and in 1 M KOH as supporting electrolyte. The kinematic viscosity of 1 M KOH at 25°C is 0.01073 cm^2/s, the diffusion coefficient of $Fe(CN)_6^{3-}$ in 1 M KOH at 25°C is 7.9×10^{-6} cm^2/s and the width of the inner ring is 0.115 cm. Figure 2 shows that δ at the inner ring for $i_{H_2} = 1$ A/cm^2 is 7.5×10^{-3} cm.

Calculation with (13) gives $U = 0.38$ cm/s. With $Re = U1/\nu$, Re is about 4. From this very low value for Re it follows that the flow in the neighbourhood of the ring electrodes is laminar.

Figures 2 and 3 show that for experiments with the hydrogen evolving disc electrode all the curves of the plots of log δ at the ring electrode *vs* log i_{H_2} at the disc electrode, are practically parallel to one another. Moreover, the slope of these curves is of the order of magnitude of those of the log δ/log i_{H_2} curve for the disc electrode.

From the experiments with electrode B it is found that δ at the inner ring is smaller than δ at both other rings for individual polarization of the rings (Fig. 3). The width of the rings of electrode B are nearly equal. Consequently, δ at the ring electrodes increases with increasing distance from the gas evolving disc electrode. This conclusion is supported by the experiments with electrode A (Fig. 2). The results of the experiments with oxygen evolution at $i_{O_2} < 20$ mA/cm^2 support the conclusions deduced from those with hydrogen evolution. However, for oxygen evolution at $i_{O_2} > 20$ mA/cm^2 the results of Figs 5 and 6 and that of Fig. 7 are completely different. In this current density range coalescence of oxygen bubbles occurs very frequently.

In the following the experiments with $i_{O_2} > 20$ mA/cm^2 are discussed. The log δ/log i_{O_2} curve at the gas evolving disc electrode (Fig. 7) is much steeper than the curves for the relation between log δ at the ring electrode and log i_{O_2} at the disc electrode (Figs 5 and 6).

Even δ at the inner ring of electrode A remains practically constant with increasing rate of oxygen evolution at the disc of electrode A. The log δ/log i_{O_2} curve at the gas evolving disc electrode agrees with those mentioned in the literature[2, 3].

From the preceeding discussion it follows that there is only an evident correlation between δ at the ring electrodes and δ at the gas evolving disc electrode if no coalescence of gas bubbles occurs. The thickness of the diffusion layer at a gas evolving electrode is then determined by the solution flow at the electrode which is induced by ascending gas bubbles. Incorporating this solution flow is basic to the hydrodynamic model introduced by Janssen and Hoogland[3].

The hydrogen evolving electrode at 1 mA/cm^2 $< i_{H_2} <$ 100 mA/cm^2 in alkaline solution generates bubbles with a practically constant diameter[3]; coalescence of bubbles does not occur. Though no measurements at $i_{H_2} > 100$ mA/cm^2 are known, the observed dependency of δ on i_{H_2} at a hydrogen evolving electrode (Fig. 4) tends to the conclusion that it is likely that at 100 mA/cm^2 $< i_{H_2} <$ 1 A/m^2 practically no coalescence of hydrogen bubbles occurs.

The experimental slope of the log δ/log i_{H_2} curve at the hydrogen evolving disc electrode is about -0.32 (Fig. 7). This value agrees with earlier results[2, 3].

For the hydrodynamic model presented in Section 4 the theoretical slope of the log δ/log v curve is equal to -0.33 at a constant uniform bubble size. Taking into consideration the assumptions made, there is a good agreement between the experimental and the theoretical slope. Consequently, the hydrodynamic model describes the mass transfer at a gas evolving electrode at which no coalescence of bubbles occurs very well.

The assumption about the size of bubbles is supported by new experimental results[21].

The bubbles formed at a hydrogen evolving electrode at which no coalescence of bubbles occurs can be divided into two groups, *viz* small bubbles forming part of a bubble train departing from an active site, and large single bubbles which grow during a relatively long time and then detach individually from the electrode.

For a hydrogen evolving electrode in alkaline solution the distribution of active sites and the ratio between the number of small bubbles and the number of large single bubbles depend on the time of polarization. At the beginning of the polarization relatively numerous single bubbles are formed and this number decreases with increasing time of polarization. In the steady state only small bubbles occur which become incorporated into bubble trains. These small bubbles have a near-uniform size, which is almost independent of current density.

REFERENCES

1. H. Vogt, Thesis, Stuttgart (1977).
2. L. J. J. Janssen, *Electrochim. Acta* **23**, 81 (1978).
3. L. J. J. Janssen and J. G. Hoogland, *Electrochim. Acta* **18**, 543 (1973).
4. J. Venczel, Thesis, Zürich (1961).
5. N. Ibl, *Chemie-Ingr.-Tech.* **35**, 353 (1963).
6. N. Ibl and J. Venczel, *Metalloberfläche* **24**, 365 (1970).
7. N. Ibl, E. Adam, J. Venczel and E. Schalch, *Chemie-Ingr.-Tech.* **43**, 202 (1971).
8. J. M. Kolthoff and E. B. Sandell, *Textbook of Quantitative Inorganic Analysis*, MacMillan, New York (1952).
9. A. J. Arvia, S. L. Marchiana and J. J. Podestá, *Electrochim. Acta* **12**, 259 (1967).
10. C. J. West, *International Critical Tables*, 5, 17. McGraw-Hill, New York, London (1933).
11. A. A. Wragg, *Electrochim. Acta* **13**, 2159 (1968).
12. C. R. Wilke, C. W. Tobias and M. Eisenberg, *Chem. Engng Prog.* **49**, 663 (1953).

13. C. R. Wilke, M. Eisenberg and C. W. Tobias, *J. electrochem. Soc.* **100**, 513 (1953).
14. R. B. Bird, W. E. Stewart and E. N. Lightfoot, *Transport Phenomena*, Wiley, New York (1963).
15. N. Ibl, *Chemie-Ingr.-Tech.* **43**, 202 (1971).
16. N. Ibl, R. Kind and E. Adam, *An. Quim.* **71**, 1008 (1975).
17. E. Weder, *Chemie-Ingr.-Tech.* **39**, 914 (1967).
18. K. Rietema and J. J. M. Rypkema, *Chem. Techniek* **2**, Ch 15 (1966).
19. N. Zuber, *Int. J. Heat Mass Transfer* **6**, 53 (1963).
20. R. N. Adams, *Electrochemistry of Solid Electrodes*, p. 76. Marcel Dekker, New York (1969).
21. R. M. de Jonge, private communication.